



HAL
open science

Behaviour of minerals during the vacuum concentration of dairy ultrafiltration permeates

Gaëlle Tanguy, Eric Beaucher, Anne Dolivet, Ali Kerjough, Marie-Bernadette Maillard, Pascaline Hamon, Thomas Croguennec

► **To cite this version:**

Gaëlle Tanguy, Eric Beaucher, Anne Dolivet, Ali Kerjough, Marie-Bernadette Maillard, et al.. Behaviour of minerals during the vacuum concentration of dairy ultrafiltration permeates. *International Dairy Journal*, 2022, 133, 10.1016/j.idairyj.2022.105426 . hal-03703706

HAL Id: hal-03703706

<https://hal.inrae.fr/hal-03703706v1>

Submitted on 24 Jun 2022

HAL is a multi-disciplinary open access archive for the deposit and dissemination of scientific research documents, whether they are published or not. The documents may come from teaching and research institutions in France or abroad, or from public or private research centers.

L'archive ouverte pluridisciplinaire **HAL**, est destinée au dépôt et à la diffusion de documents scientifiques de niveau recherche, publiés ou non, émanant des établissements d'enseignement et de recherche français ou étrangers, des laboratoires publics ou privés.



Distributed under a Creative Commons Attribution - NonCommercial - NoDerivatives 4.0 International License



Behaviour of minerals during the vacuum concentration of dairy ultrafiltration permeates



Gaëlle Tanguy^{*}, Eric Beaucher, Anne Dolivet, Ali Kerjough, Marie-Bernadette Maillard, Pascaline Hamon, Thomas Croguennec

STLO, INRAE, INSTITUT AGRO, 35042 Rennes, France

ARTICLE INFO

Article history:

Received 30 November 2021
Received in revised form
24 May 2022
Accepted 28 May 2022
Available online 3 June 2022

ABSTRACT

Whey concentration using evaporators results in deposit of matter on the hot surfaces of the evaporation tubes. The mass deposited during concentration depends mainly on the mineral composition of the whey, which varies considerably depending on the production process. We investigated the behaviour of ultrafiltration permeates (UFP) during concentration and the susceptibility of their mineral fraction to precipitation. UFP with differing mineral compositions were produced by acidification of milk with different acids to pH values between 4.6 and 6.3, followed by ultrafiltration. The results revealed either no precipitation or the precipitation of calcium salts (calcium phosphate, calcium citrate) in the concentrates. The behaviour of mineral fraction during concentration could be assessed by considering: (i) the nature and quantities of cations and anions in the concentrates, (ii) the anionic forms present at the pH of the concentrates and their association constants with calcium, and (iii) the solubility limit of calcium salts.

© 2022 Elsevier Ltd. All rights reserved.

1. Introduction

Whey, the serum phase of milk, is a co-product of cheese and casein manufacture in the dairy industry. It is the liquid fraction that remains after the enzymatic coagulation of milk, its microbial fermentation or the addition of mineral/organic acid (Smithers, 2008; Zall, 1992). In addition, 96% of whey comes from cheese-making manufacture and the rest from that of casein (Ganju & Gogate, 2017). In the dairy industry it is usual to classify whey in two major categories depending on the manufacturing process; namely sweet whey and acid whey. Sweet whey is produced during the manufacture of enzymatic-type cheeses such as Cheddar and Swiss cheese whereas acid whey is generated during that of acid-coagulated dairy products such as fresh cheese, cottage cheese and strained yoghurt (Ganju & Gogate, 2017; Schmidt, Packard, & Morris, 1984).

Whey contains a large quantity of water, lactose, nitrogen compounds (soluble proteins, peptides, amino acids) and varying amounts of minerals, particularly calcium, phosphate, sodium and potassium (Gernigon et al., 2013; Schmidt et al., 1984). The

composition of whey can vary considerably and mainly depends on seasonal variations and the cheese manufacturing process (Schmidt et al., 1984). Compared with sweet whey, acid whey has a much lower pH; it contains less protein and lactose but has a higher mineral content, particularly of calcium, phosphate and lactic acid (Schmidt et al., 1984; Schuck et al., 2004; Zall, 1992). This results in significant differences in the sensory, nutritional and technological properties of whey but also influences the processing of whey streams and the quality of the resulting products (Pearce, 1992).

Sweet whey is now efficiently processed into a variety of food ingredients (beverage powders, bakery items, ice creams); for example, sweet whey is converted into non-sticky free flowing powders using concentration by vacuum evaporation up to a 500–600 g kg⁻¹ dry matter (DM) content, lactose crystallisation in tanks and subsequent spray drying (De Wit, 2001). By contrast, acid whey is considered a difficult product to process, mainly because of its high mineral content, low lactose content and markedly variable composition (Saulnier, Calco, Humbert, & Linden, 1996; Schuck et al., 2004). It has been evidenced during the manufacturing of acid whey powders that the high lactic acid and calcium contents hinder the correct crystallisation of lactose, which remains in its amorphous form. This in turn affects the spray-drying operation and the properties of the resulting powder (Wijayasinghe, Vasiljevic, & Chandrapala, 2016).

^{*} Corresponding author.

E-mail address: gaelle.tanguy@inrae.fr (G. Tanguy).

Whey is concentrated using vacuum evaporation, either to reduce storage and transportation costs (concentration up to 300 g kg⁻¹ DM) or to ease further processing such as lactose crystallisation and spray-drying (concentration from 250 to 600 g kg⁻¹ DM, depending on the composition of the concentrate) (Pearce, 1992). This operation is carried out in falling-film evaporators. The equipment consists of a bundle of vertical tubes in which a thin film of product flows down onto the inner tube surfaces in indirect contact with the heating medium (primary vapour). During vacuum concentration, the product components undergo numerous changes that in turn affect the biochemical, physical and rheological properties of the product (Singh & Newstead, 1992; Walstra, Wouters, & Guerts, 2006). The behaviour of the mineral fraction is difficult to predict because phenomena with sometimes opposite effects occur in the products. For instance, the solubility limit of some salts, such as calcium phosphate and calcium citrate, may be exceeded during increasing ion concentration. The precipitation of calcium salts releases H⁺ that lowers the pH of the concentrated solution. In the meantime, the greater ion concentration of the concentrates increases the ionic strength which in turn reduces ion activity coefficients, increasing salt solubility (Walstra et al., 2006).

One undesirable effect of salt precipitation is the deposition of matter on the hot surfaces of falling film evaporators. This phenomenon, defined as fouling, is a major problem in the dairy industry as it affects both product quality and processing efficiency. Fouling causes a reduction in heat transfer coefficients and requires more frequent cleaning of the evaporators. It generates product losses and increases both operating costs and environmental impact (Daufin & Labbé, 1998; de Jong, 1997). Unlike heat-exchangers, few studies have focused on the fouling of falling-film evaporators, but it is generally agreed that the deposit composition in falling-film evaporators differs from that seen in heat-exchangers (Jeurnink & Brinkman, 1994; Morison, 2015). Jeurnink and Brinkman (1994) evidenced the compositional differences of the deposits in heat-exchangers and falling-film evaporators at an industrial scale during the concentration of milk and whey. Further, they showed that the main components in the deposit were proteins and calcium phosphate after whey concentration from 50 to 280 g kg⁻¹ DM, while it was calcium citrate after whey concentration from 280 to 550 g kg⁻¹ DM. Similarly, Vavrusova, Johansen, Garcia, and Skibsted (2017a) evidenced the predominance of calcium citrate tetrahydrate in the deposit after whey concentration. Calcium phosphate was also present, but to a lesser extent. Lastly, Kessler (1986) showed that the composition of the deposit was closely dependent on the pH of acid whey; he stated that the proportion of minerals in the deposits would be greater at high pH values and high mineral concentrations.

Tanguy et al. (2016, 2019) also conducted experiments at the pilot scale to determine the nature of the fouling deposit formed during the concentration of milk ultrafiltrate, milk microfiltrate, hydrochloric acid whey and lactic acid whey. Briefly, these studies showed that (i) calcium phosphate was the main component in the deposit when concentrating milk ultrafiltrate, (ii) proteins reduced the amount of deposit when concentrating milk microfiltrate, and (iii) the deposit formed when concentrating hydrochloric acid whey was composed of calcium citrate whereas no deposition was observed when concentrating lactic acid whey.

To improve our understanding of the fouling process and the subsequent cleaning of evaporators, it would be beneficial to generalise the previous results and predict how the mineral fraction of whey will behave during concentration. However, it would be relatively difficult to start using industrial whey because of its variable composition in minerals and other components. A potential strategy was therefore to modify the mineral composition of the same starting raw material.

During this study, we therefore investigated the degree to which the mineral composition and initial pH influenced the nature and amount of precipitate formed when concentrating different milk permeates, this precipitate being likely to deposit on the inner surface of tubes in evaporators. Permeates with varying mineral compositions and pH were prepared by the ultrafiltration of non-acidified (pH 6.7; control milk) and acidified milk at pH values of between 6.3 and 4.6. The type of acid used for milk acidification (hydrochloric, citric and lactic) and the final pH of the permeates were chosen to prepare products that would simulate the mineral composition of the whey produced during cheese manufacture (hard-type or soft-type cheeses) and acid casein production. However, it should be stressed that these ultrafiltration permeates differed substantially from real whey in terms of their higher content in citrate (not consumed by bacteria) and lower level of proteins (removed using ultrafiltration). The permeates were then concentrated at DM contents ranging from 45 to 500 g kg⁻¹. The mineral composition of the concentrates and the distribution of the minerals between the soluble phase and precipitate were then determined to understand the behaviour of the mineral fraction during concentration.

2. Materials and methods

2.1. Preparation of milk permeates

The processing scheme to prepare milk permeates (Fig. 1) was defined in line with the work of Mekmene et al. (2012). Thermised skimmed milk was divided into six batches; five of these were acidified at 4 °C under agitation with lactic, hydrochloric or citric acid (VWR, Fontenay-sous-Bois, France) up to pH values representative of the whey drained during the manufacture of cheese and acid caseins. Preliminary tests were conducted to determine the quantity of acid required to reach the target pH during milk acidification. The concentrations of acid solutions were then adjusted so that the milk samples would be diluted similarly (dilution factor of 2.5%, w/w), the control milk at pH 6.7 being diluted with demineralised water. Acidified milk samples were kept overnight at 4 °C.

Non-acidified milk and acidified milk were warmed and stored at 25 °C for 2 h to reach mineral equilibrium before ultrafiltration. The milk was coarsely filtered to remove any large flocs and then ultrafiltered at 25 °C through tubular ceramic membranes (total membrane area of 2 × 0.36 m²; cut-off 15 kDa, Membralox, EP1960, Pall, Bazel, France) set on a TIA pilot (Bollène, France). The permeates were collected, filtered using a 0.45 µm PES membrane sterile filter unit (Nalgene, Thermo Fischer Scientific, Waltham, USA) and stored at 4 °C in 1-L bottles.

2.2. Vacuum concentration of permeates

The permeates were concentrated using rotary evaporators (Hei-VAP Value Digital, Heidolph Instruments, Schwabach, Germany) at an absolute pressure of between 10.1 and 16.5 kPa, which corresponds to evaporation temperatures within the range 46–56 °C. The rotation speed of the 1-L evaporation flask was 120 rpm. The permeates were concentrated at four different concentration factors (CF) ranging from 3.1 to 12.7. For each CF, the initial volume of permeate in the evaporation flask was adjusted to obtain about 100 mL of concentrate at the end of the experiment for further analysis. The experiments were performed in duplicate, more especially during two experimental series referred to as set #1 and set #2. A sample of permeate before concentration (named CF1) was saved from each series. In total, concentration of the permeates was studied at 10 experimental points, except P-AL3. In

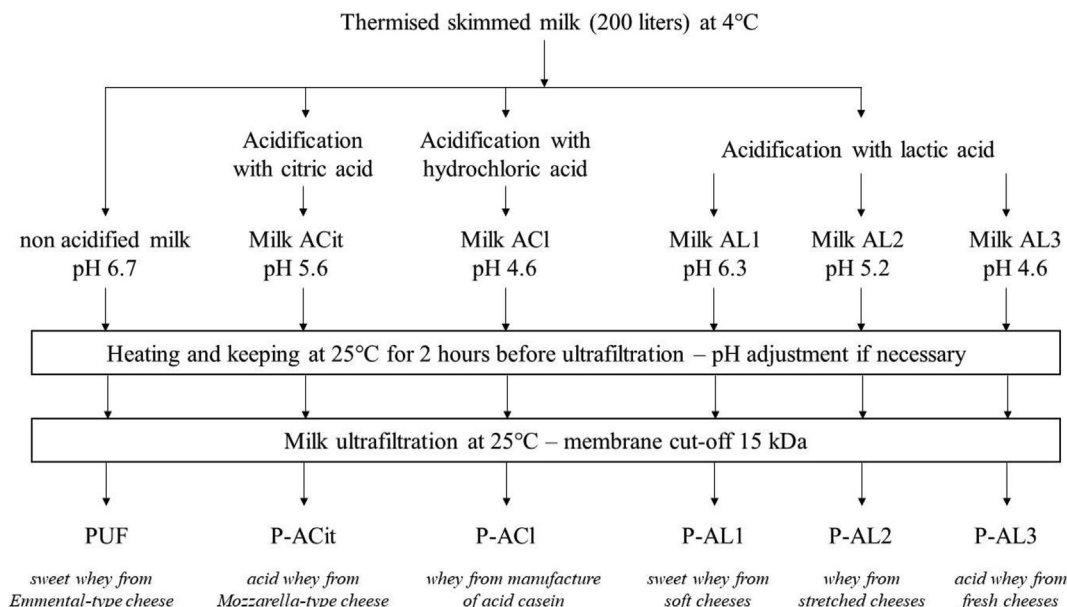


Fig. 1. Processing scheme for the preparation of milk permeates from non acidified milk (pH 6.7) and milks acidified at different (pH 4.6–6.3) with different acids (citric, hydrochloric and lactic). In italics: wheys produced from the manufacture of cheese and acid caseins for which each model cheese whey is representative.

the latter case, only six points were available because four samples were contaminated and not appropriate for experimentation. The duration of the experiments ranged from 1 to 4 h depending of the expected CF. Images of the concentrates were taken on the day of the experiment, up to 3 h after the end of the concentration step.

2.3. Characterisation of permeates and concentrates

For each sample, the pH was measured and the soluble phase separated from the precipitated phase (method described below) immediately after vacuum concentration in the rotavapors. In addition, the concentrates and their respective soluble phases were diluted with demineralised water to a dry matter content comparable with that of the initial permeate to enable quantitative determination of the ash, total protein and total ion contents.

2.3.1. pH

The pH of permeates and concentrates was measured at 25 °C using a pH meter (HI 9024 microcomputer pH meter, Hanna Instruments, Romania). All measurements were made in duplicate. The experimental error was ± 0.02 units.

2.3.2. Dry matter content

The dry matter content of permeates and concentrates was determined as described in IDF standard 21B (ISO-IDF, 1987). Briefly, five grams of product were mixed with sand in a capsule and dried at 102 ± 2 °C in an oven for 7 h. The weight loss of the capsule before and after drying was taken as the amount of water it had contained. This analysis was performed in duplicate. The experimental error was $\pm 5\%$.

2.3.3. Total nitrogen and ash contents

The total nitrogen content of permeates and concentrates was determined using the Kjeldhal method as described in IDF standard 20B (ISO-IDF, 1993). The nitrogen content was converted to the protein content using a conversion factor of 6.38. Further, the non-casein and non-protein nitrogen contents (respectively NCN and NPN contents) of the thermised skimmed milk were determined

using the same method. The NCN corresponds to the soluble fraction at pH 4.6 and was determined after the acid precipitation of casein micelles at pH 4.6 using a 10% acetic acid solution. The NPN corresponds to the soluble fraction after the acid precipitation of milk proteins using 12% trichloroacetic acid. The experimental errors were $\pm 1\%$ for the total nitrogen content and $\pm 2\%$ for the NCN and NPN contents.

An RP-HPLC method was used to quantify α -lactalbumin and β -lactoglobulin in the permeates. The method was adapted from (Resmini, Pellegrino, Adreini, & Prati, 1989) using a PLRP-S column (polystyrene divinylbenzene gel, 30 nm, 8 μ m, 150 \times 2.1 mm; Agilent Technologies, Varian, Les Ulis, France).

The ash content was determined as described in IDF standard 27B (ISO-IDF, 1964). Ten grams of product were incinerated at 550 °C in an oven for 5 h. The analysis was performed in duplicate. The experimental error was $\pm 5\%$.

2.3.4. Concentrations of cations and anions

The contents in cations (calcium, magnesium, sodium, potassium) and anions (lactate, chloride, inorganic phosphate, citrate) were determined in the permeates and concentrates and their respective soluble phases. The soluble phases of the permeates and concentrates were obtained by ultrafiltration on an analytical membrane (molecular cut-off 10 kg mol⁻¹; Vivaspin, Palaiseau, France) at a centrifugation rate of 1800 \times g at 20 °C for 1.5 h.

The cations were quantified using inductively coupled plasma-atomic emission spectroscopy (ICP-AES) (iCAP 7200 Duo, Thermo Fisher Scientific, Waltham, USA) and the samples were diluted with a 2% (w/w) HNO₃ solution before analysis. The anions were quantified using a 930 Compact IC Flex ion chromatography system (Metrohm, Herisau, Swiss) that included a Dionex IonPacAS11 column (4 \times 250 mm) and a conductivity detector. The following conditions were used at 30 °C and 1 mL min⁻¹: gradient elution with 0.3–34 mM NaOH solution for 24 min and column re-equilibration for 15 min with 0.3 mM NaOH. Ion contents resulted from two independent samplings and each sample was analysed in duplicate. The experimental errors of ICP-AES and ion chromatography were 2% and 1%, respectively.

Changes to total and soluble ion contents during concentration were plotted on the same graph as a function of the concentrate DM content. The difference between the total and soluble ion contents corresponded to ions that precipitated in the concentrate. The experimental total ion content of the concentrate was compared with a calculated total ion content, defined as the product of the concentration factor by the experimental total ion content of the corresponding permeate.

2.4. Determination of the composition of precipitates

The precipitate composition in the concentrates with higher CFs was determined indirectly from the experimental composition of the concentrate and the corresponding supernatant obtained using centrifugation (1800×g; 20 °C; 20 min) in 50-mL plastic centrifuge tubes. Both products were characterised in terms of their DM, TN, ash and total ion contents using the methods described previously. In addition, the lactose content was quantified using a ICS-5000+ Dionex ion chromatography system (Thermo Electron SA, Courtaboeuf, France) that included a CarboPac PA210-4 µm column (2 × 150 mm) and amperometric detector. The following conditions were used at 30 °C and 0.2 mL min⁻¹: isocratic elution with 13 mM KOH for 32 min followed by flush out with 100 mM KOH for 23 min and column re-equilibration for 10 min with 13 mM KOH. A solution containing lactose (Sigma) at 0.1, 0.25, 0.5, 1, 2.5, 5, 10, 20 and 40 mg L⁻¹ was used as a standard. The analytical results enabled an estimate of the percentage of precipitate in the different concentrates, as well as their composition.

3. Results and discussion

3.1. Composition of permeates

The composition of the permeates is given in Table 1. The mineral composition of the permeate resulting from milk ultrafiltration (PUF) was close to the lower end of the values commonly reported (Gaucheron, Le Graët, Piot, & Boyaval, 1996; Le Graët & Brule, 1993; Walstra et al., 2006). Similarly, the mineral compositions in PUF, P-ACI, P-AL2 and P-AL3 were within the range of those reported by Mekmene et al. (2012).

The acidification of milk prior to ultrafiltration led to the solubilisation of calcium and inorganic phosphate (and small

quantities of magnesium and citrate) associated with casein micelles, and their subsequent transfer to the soluble phase of milk (Gaucheron, 2005). As a consequence, the calcium and inorganic phosphate contents (magnesium and citrate contents to a lesser extent) in the permeates increased as the pH decreased.

As expected, the acidification of milk with citric, hydrochloric or lactic acid induced higher citrate, chloride and lactate contents in the resulting permeates (P-ACit, P-ACI, P-AL1 to P-AL3, respectively).

The TN content of permeates was composed of the non-protein content of milk (1.60 g kg⁻¹) and some remaining soluble proteins. β-lactoglobulin and α-lactoglobulin levels were within the range 0.141–1.318 g kg⁻¹ and 0–0.429 g kg⁻¹, respectively. Both proteins were found in smaller quantities in P-AL2 (pH 5.25) compared with the other permeates. At this pH, milk was flocculated and more drastic sieving was required to recover the soluble phase, thus explaining the greater retention of protein. By contrast, β-lactoglobulin and α-lactoglobulin were found at higher levels in P-ACI and P-AL3, indicating that the ultrafiltration membranes became more leaky at low pH values (4.64 ± 0.02).

3.2. Evolution of the pH of concentrates during concentration

The pH of the concentrates fell during concentration (Fig. 2) due to the rise in ion concentrations that favoured the precipitation of poorly soluble salts, especially calcium phosphate. Gao et al. (2010) had suggested this as the main reason for the fall in pH in simulated milk ultrafiltrate (SMUF) after adding CaCl₂ (i.e., a higher content in free Ca²⁺). The added Ca²⁺ interacted with HPO₄²⁻ to form amorphous CaHPO₄·2H₂O that was converted into its crystalline form, and HPO₄²⁻ was regenerated by the deprotonation of H₂PO₄⁻ causing a reduction in pH.

In concentrates in which calcium phosphate precipitation did not occur – or only at a high CF – the fall in pH during concentration might have been related to the formation of other calcium salts such as calcium citrate that precipitated and led to the deprotonation of HCit²⁻, as well as an increase in ionic strength that subsequently lowered the ion activity coefficients. Lastly, even if P-AL3 and P-ACI permeates had the same initial pH (around 4.6), the pH decrease in P-AL3 was limited throughout concentration when compared with P-ACI. This might have been caused by less precipitation of calcium salts and the presence of lactate which contributed to the buffering capacity of the concentrates.

Table 1
Composition of permeates obtained from ultrafiltration of nonacidified and acidified milk.^a

Parameter	PUF	P-ACit	P-ACI	P-AL1	P-AL2	P-AL3
pH	6.89 ± 0.01	5.72 ± 0.01	4.64 ± 0.00	6.34 ± 0.01	5.21 ± 0.04	4.63 ± 0.00
DM (g kg ⁻¹)	47.5 ± 0.3	43.2 ± 0.2	52.8 ± 0.4	48.2 ± 0.3	42.3 ± 0.2	54.4 ± 0.0
Ash (g kg ⁻¹)	4.3 ± 0.1	5.2 ± 0.1	6.7 ± 0.1	4.4 ± 0.4	6.0 ± 0.1	6.5 ± 0.0
TN (g kg ⁻¹)	1.9 ± 0.1	1.9 ± 0.1	3.3 ± 0.1	1.9 ± 0.1	1.5 ± 0.1	3.1 ± 0.0
α-Lactalbumin (g kg ⁻¹)	0.115	0.110	0.429	0.115	0	0.381
β-Lactoglobulin (g kg ⁻¹)	0.228	0.300	1.318	0.272	0.141	1.230
Casein (g kg ⁻¹)	abs	abs	abs	abs	abs	abs
Ca (mmol kg ⁻¹)	9.0 ± 0.9	18.4 ± 0.2	31.2 ± 3.0	16.1 ± 0.3	23.6 ± 0.1	29.8 ± 0.1
Mg (mmol kg ⁻¹)	2.3 ± 0.0	2.9 ± 0.0	3.9 ± 0.0	2.7 ± 0.0	3.2 ± 0.0	3.7 ± 0.0
Na (mmol kg ⁻¹)	11.8 ± 1.4	11.1 ± 1.0	13.1 ± 0.3	11.9 ± 1.2	12.6 ± 0.4	12.3 ± 0.0
K (mmol kg ⁻¹)	33.4 ± 0.5	33.6 ± 1.1	38.4 ± 0.4	35.5 ± 0.3	35.9 ± 1.0	37.6 ± 0.1
Lactate (mmol kg ⁻¹)	abs	abs	abs	11.1 ± 0.4	39.8 ± 2.2	59.7 ± 0.1
Cl (mmol kg ⁻¹)	26.7 ± 0.2	26.5 ± 0.2	71.2 ± 1.1	26.4 ± 0.2	24.6 ± 0.1	24.1 ± 0.6
Pi (mmol kg ⁻¹)	8.3 ± 0.2	15.4 ± 0.4	17.3 ± 0.2	10.3 ± 0.1	16.3 ± 0.1	17.1 ± 0.0
Citrate (mmol kg ⁻¹)	6.2 ± 0.1	11.9 ± 0.1	7.4 ± 0.1	6.4 ± 0.6	6.0 ± 0.1	7.3 ± 0.0

^a Abbreviations are: Pi, inorganic phosphate (includes inorganic phosphate in the soluble phase and inorganic phosphate transferred from micellar to soluble phase due to dissociation of micellar calcium phosphate, resulting from milk acidification); abs, absence.

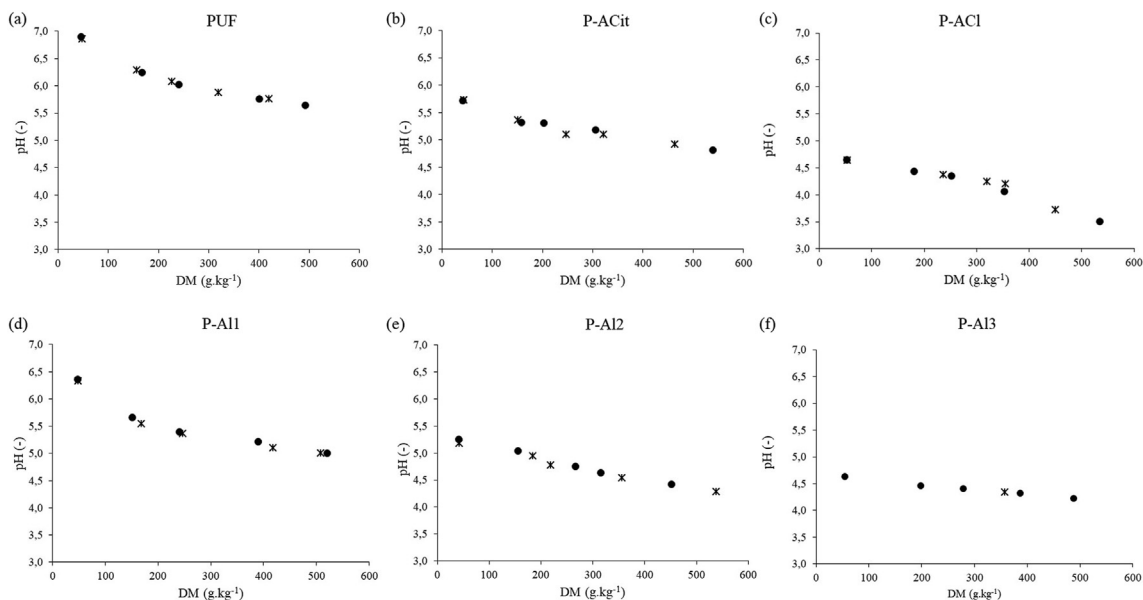


Fig. 2. Evolution of pH of concentrates during vacuum concentration of (a) PUF, (b) P-ACit, (c) P-ACI, (d) P-AL1, (e) P-AL2 and (f) P-AL3; ●, set #1 and ✱, set #2, representing the 2 series of concentration experiments.

3.3. Aspect of concentrates and the coarse composition of resulting precipitates

The concentrates became increasingly turbid as the concentration rose and a precipitate appeared gradually at the bottom of the sample bottles (Fig. 3). Although the initiation of the precipitation is time-dependent, and particularly close to the solubility limit, and the observed precipitates were probably not complete when the images were captured, we noted that the CF at which the precipitate appeared was dependent on the composition of the permeate. For instance, a precipitate appeared from CF 3.5 in PUF concentrates whereas it was observed later in P-AL3 concentrates (from CF 7.1).

The composition of the precipitates that formed in the concentrates at the highest CF was determined by analysing the global composition of the concentrates and corresponding supernatants after centrifugation. The main drawback of this indirect method was that it produced some inconsistent results, such as negative concentrations and dry matter contents over 1000 g kg^{-1} . However, it provided the coarse composition of the precipitates and evidenced the nature of the ions that precipitated in the concentrates.

Although the concentrates had variable CF values ranging from 8.6 to 10.7, it appeared that the P-AL1 concentrate contained much

more precipitate than the others (Table 2), at 24.7 g per 100 g of P-AL1, whereas PUF, P-ACI and P-ACit contained only 8.9, 6.0 and 10.7 g of precipitate, respectively. In all precipitates at the end of concentration, the principal component was lactose which accounted for more than 80 g per 100 g precipitate. The higher level of lactose in the P-AL1 precipitate indicated that the physico-chemical conditions in this concentrate favoured lactose crystallisation when compared with other concentrates such as PUF and those resulting from milk acidification using hydrochloric acid and citric acid. Lactate ions may be the promoting agent of lactose crystallisation. This hypothesis had been confirmed in the work of Gernigon et al. (2013) and Smart and Smith (1992) who evidenced the accelerating effect of lactate on lactose crystallisation, and in particular on crystal growth.

Apart from lactose, the nature and quantity of the ions precipitated depended on the type of permeate. The main mineral components in the PUF precipitate were calcium and phosphate (52 and 26 mmol per 100 g precipitate, respectively) (Table 2). Citrate was also present but to a lesser degree. Unlike the PUF concentrate, calcium and citrate were the main compounds found in P-ACit (150 and 88 mmol 100 g^{-1} , respectively) whereas phosphate was seen in smaller quantities. Lastly, calcium and citrate remained the main

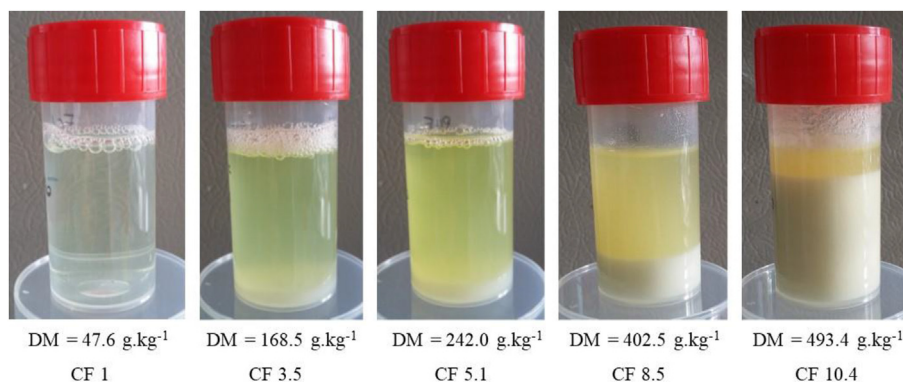


Fig. 3. Pictures of concentrates produced during concentration of PUF from CF 1 to CF 10.4 (set #1).

Table 2

Estimation of the composition of the precipitate deduced from the experimental analysis of the more concentrated permeates (set #2) and the corresponding supernatant after centrifugation.^a

Parameter	PUF CF 8.9	P-ACI CF 8.6	P-ACit CF 10.7	P-AL1 CF 10.6
Mass of precipitate	8.9	6.0	10.7	24.7
Composition of precipitate				
DM (g)	101.8	105.2	111.3	92.0
TN (g)	0.6	7.2	3.6	3.0
Ash (g)	4.4	10.6	9.5	0.5
Lactose (g)	100.2	79.9	87.2	96.7
Calcium (mmol)	52	127	150	17
Lactate (mmol)	0	0	2	2
Inorganic phosphate (mmol)	26	27	5	13
Citrate (mmol)	3	50	88	3

^a Centrifugation was at 1800×g, 20 min, 20 °C; mass of precipitate was per 100 g of concentrate, composition of precipitate is given per 100 g of precipitate.

compounds in P-ACI precipitates (127 and 50 mmol 100 g⁻¹, respectively) but quite a large quantity of phosphate was present (27 mmol 100 g⁻¹). The mineral fraction in the P-AL1 concentrate was very low with an ash content equal to 0.5 g 100 g⁻¹ precipitate. It contained some calcium, phosphate and citrate (17, 13 and 3 mmol 100 g⁻¹), but only 2 mmol 100 g⁻¹ of lactate were evidenced.

Follow-up of the soluble ion contents during concentration showed that some of them remained soluble whatever the permeate and CF. This was the case for monovalent ions (Na⁺, K⁺ and Cl⁻) that existed mainly as free ions in the soluble phase of permeates and remained soluble in the concentrates, even in the most concentrated (Table 3). Further, although Mg²⁺ has a strong affinity for citrate and phosphate ions, we could not find any evidence of magnesium insolubilisation during concentration. On the contrary, an increasing part of the soluble calcium, citrate and phosphate ions became insoluble during concentration (Figs. 4 and 5) but the nature of the precipitate, and the CF at which precipitation appeared, depended on the type of permeate.

3.3.1. PUF concentration

During PUF concentration, some calcium phosphate precipitated first and at a level higher than 400 g kg⁻¹ DM, some citrate contributed to the precipitate (Fig. 4). In the soluble phase of milk at pH 6.6–6.7, calcium is mainly present as a soluble complex with citrate, as free ionic Ca²⁺ and to a lesser extent associated with inorganic phosphate and chloride (Gaucheron, 2005). It should be noted that calcium phosphate (which has a solubility limit of 0.6 mmol L⁻¹) was at the edge of precipitating. In addition, the amount of phosphate ions, in the ionic form HPO₄²⁻, was almost ten times that of free citrate ion in PUF at pH 6.6–6.7. Their contents have been estimated at 2.65 and 0.26 mM, respectively (Gaucheron, 2005). These conditions were favourable to calcium phosphate precipitation in PUF concentrates. At higher concentrations, the solubility limit of calcium citrate might in turn be exceeded and its precipitation might add to that of calcium phosphate. Our results

were in line with those of a previous experimental study carried out at pilot-scale by Tanguy et al. (2016). They also agreed well with theoretical calculations performed using MilkSalt GLM®, a software developed by Mekmene, Le Graët, and Gaucheron (2009, 2010) that predicts ion distribution in milk, where calculations are based on the affinities between cations (calcium, sodium, potassium and magnesium) and anions (inorganic phosphate, chloride, citrate and lactate) and calcium phosphate saturation. The input data are the total ion contents and the pH value. For instance, for the more concentrated PUF at CF 10.4, the experimental concentrations of calcium and phosphate precipitated were equal to 62 and 38 mM, which were close to the theoretical values determined by the software, at 62 and 34 mM, respectively. Finally, these results could be related to the work by Garcia, Vavrusova, and Skibsted (2018) who studied the dynamic exchange between calcium phosphate and calcium citrate from an equimolar (0.10 mol L⁻¹) mixture of calcium chloride, sodium citrate and sodium phosphate. In that case, the time-dependent pH fell from 6.3 to 4.0 over 48 h due to calcium phosphate precipitation. With this decrease in the pH, a slow precipitation of calcium citrate (Ca₃Cit₂) started. Moreover, the calcium phosphate precipitate formed initially gradually solubilised with a decreasing pH. The precipitation of calcium citrate in the PUF concentrate at a high CF and low pH was in agreement with this explanation.

3.3.2. P-ACit concentration

The experimental results indicated that only calcium citrate salt was formed during the concentration of P-ACit. Moreover, calcium citrate precipitation was observed early in the concentration process, as from about 150 to 250 g kg⁻¹ DM (Fig. 4). Finally, large quantities of calcium and citrate ions were precipitated at high dry matter contents (about 80% of calcium and 75% of citrate ions at around 500 g kg⁻¹ DM). On the other hand, the evolution of total and soluble phosphate ion contents indicated that all phosphate ions remained soluble throughout the concentration process. A large quantity of citrate ions (11.9 mmol kg⁻¹ compared with a

Table 3

Total and soluble sodium, potassium, chloride and magnesium ion contents in the more concentrated permeate concentrates.

Ionic species (mmol kg ⁻¹)	PUF concentrate CF 10.4		P-ACit concentrate CF 12.5		P-ACI concentrate CF 10.1		P-AL1 concentrate CF 10.8		P-AL2 concentrate CF 12.7		P-AL3 concentrate CF 9.0	
	total	soluble	total	soluble	total	soluble	total	soluble	total	soluble	total	soluble
Na	127	103	120	137	119	113	110	117	154	185	110	107
K	344	341	399	403	375	357	371	368	443	488	339	333
Cl	283	281	329	332	730	706	288	285	313	337	216	213
Mg	25	22	35	32	41	38	28	26	41	43	34	33

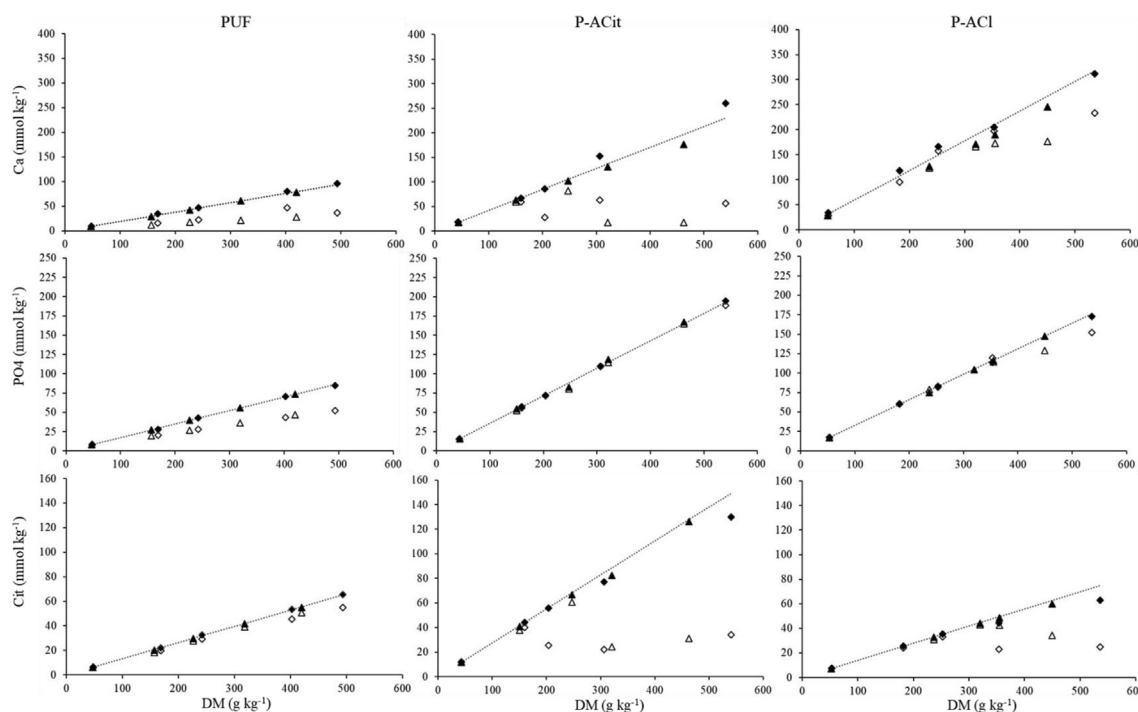


Fig. 4. Evolution of total and soluble calcium, inorganic phosphate and citrate contents during concentration of PUF, P-ACit and P-ACI permeates. Set #1 and set #2 represented the 2 series of concentration experiments. Dark and white diamonds are relative respectively to experimental total (\blacklozenge) and soluble (\circ) ion contents for set #1. Dark and white triangles are relative respectively to experimental total (\blacktriangle) and soluble (\triangle) ion contents for set #2. Dotted line referred to calculated total ion content.

mean value of 6.7 mmol kg^{-1} in other permeates) was added during milk acidification with citric acid. Meanwhile, the pH of the milk fell from 6.8 to 5.7, leading to the dissolution of micellar calcium phosphate and a subsequent increase in the concentrations of calcium and phosphate ions in the soluble phase. As a result, the initial concentrations of calcium, phosphate and citrate ions in the P-ACit permeate reached 18, 15 and 12 mM.

The results obtained during P-ACit concentration could be related to the works of Rice, Barber, O'Connor, Stevens, and Kentish (2010) who studied calcium speciation and calcium salt precipitation in a dairy ultrafiltration permeate using both experimental data and theoretical calculations. In a predicted equimolar (2 mM) calcium-phosphate-citrate system, they showed that calcium speciation preferentially formed calcium citrate salts whereas few calcium phosphate salts developed. The model predicted that calcium ions were mainly free (65%) in the complex form of CaCit^- (30%) and CaHCit (5%) at pH 5.7. At a lower pH, the percentage of CaHCit and free Ca^{2+} increased whereas that of CaCit^- decreased. In P-ACit, the addition of citrate inhibited calcium phosphate precipitation due to the strong chelating capacity of citrate with calcium and the resulting formation of CaCit^- , the ionic calcium available for calcium phosphate precipitation being reduced. It also induced a shift of the saturation ratios of calcium phosphate salts, HAP (hydroxyapatite) and OCP (octacalcium phosphate) to higher pH values and further reduced the likelihood of calcium phosphate precipitation. Rice et al 2010 added that in real dairy ultrafiltration permeates, other compounds such as magnesium might form a magnesium phosphate complex, reducing the phosphate ions available for calcium phosphate precipitation.

Several authors have stated that the rate of calcium citrate precipitation was slow (Garcia et al., 2018; Liu, Kirkensgaard, & Skibsted, 2021; Vavrusova, Garcia, Danielsen & Skibsted, 2017b). Garcia et al. (2018) mentioned that the solutions remained clear for hours before the precipitation of calcium citrate became visible,

and even if the solution was supersaturated. According to our results, the precipitation of calcium citrate was quite rapid since P-ACit concentration up to the higher CF lasted for only 4 h. This precipitation could be explained by the considerable supersaturation of citrate and calcium ions (Vavrusova et al., 2017b) and/or a facilitated nucleation by "impurities" such as the lactose crystals in the P-ACit concentrate.

3.3.3. P-ACI concentration

The results obtained during P-ACI concentration were quite similar to those obtained during P-ACit concentration: they evidenced mainly calcium citrate precipitation and only some calcium phosphate precipitation at high DM contents (Fig. 4). In both cases, calcium citrate precipitation was seen from a citrate content close to 40 mmol kg^{-1} but due to lower citrate content in P-ACI than in P-ACit, it was observed later during P-ACI concentration, as from about 300 g kg^{-1} DM rather than $150\text{--}200 \text{ g kg}^{-1}$ for P-ACit concentration. It should be noted that on the graph showing the evolution of total and soluble citrate ion contents as a function of the DM content, it appeared that the threshold from which precipitation started was shifted slightly upwards by about 40 g kg^{-1} DM in experimental set #2 compared with experimental set #1. This slight difference could be explained by the fact that the milk salt equilibrium constitutes a dynamic system which is sensitive to minor variations in conditions such as pH, temperature or sample heterogeneity. Moreover, for some salts such as calcium citrate, there is an induction period prior to precipitation (Garcia et al., 2018).

According to the work by Rice et al. (2010), in the pH range 3.7–4.6, calcium would be mainly free (70–90%) in the complex form of CaHCit (17–28%) and CaCit^- (0–12%). Only 1–2% of calcium ions would be under the calcium salt CaH_2PO_4 . Even if HCit^{2-} has a lower affinity for calcium than Cit^{3-} (876 and $1.65 \times 10^5 \text{ M}^{-1}$, respectively, according to Holt et al. (1981), HCit^{2-} sequestered ion

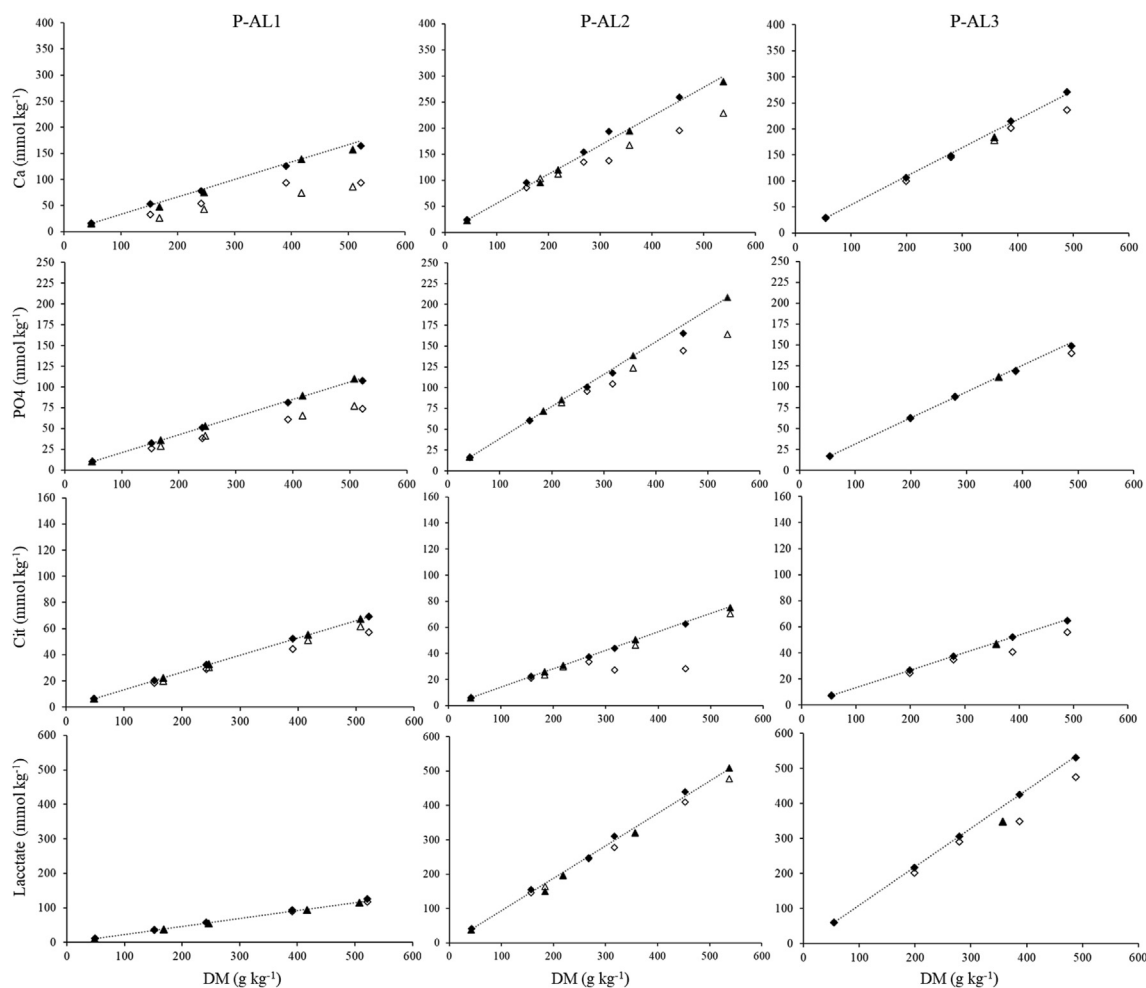


Fig. 5. Evolution of total and soluble calcium, inorganic phosphate, citrate and lactate contents during concentration of P-AL1 P-AL2 and P-AL3 permeates. Set #1 and set #2 represented the 2 series of concentration experiments. Dark and white diamonds are relative respectively to experimental total (\blacklozenge) and soluble (\circ) ion contents for set #1. Dark and white triangles are relative respectively to experimental total (\blacktriangle) and soluble (\triangle) ion contents for set #2. Dotted line refers to calculated total ion content.

calcium and reduced the part of ionic calcium available for calcium phosphate precipitation.

The results obtained during the present study were in accordance with those of a previous study carried out at the pilot scale (Tanguy et al., 2019): it was evidenced that the insoluble salt which formed in the concentrates during P-AL1 concentration was calcium citrate. However, calcium citrate precipitation started at a lower DM content (around 150 g kg^{-1}). The total calcium and citrate ion contents were close to 90 mmol kg^{-1} and 20 mmol kg^{-1} , respectively, but as mentioned previously, several parameters could affect salt solubility. Furthermore, the composition of the hydrochloric whey and the experimental conditions (pilot-scale versus lab-scale) were different in the two studies.

3.3.4. Concentration of P-AL1, P-AL2 and P-AL3

The experimental results regarding the concentration of P-AL1, P-AL2 and P-AL3 were compared with each other as the permeates differed in terms of the amount of lactic acid added and their resulting pH (pH 6.35, 5.25 and 4.63, respectively). As a consequence, larger quantities of lactate ions were present in P-AL3 and P-AL2 when compared with P-AL1. The same observation was also true for the total calcium and phosphate contents because of the pH decrease and the dissociation of micellar calcium phosphate. Meanwhile, the citrate content remained relatively constant and

close to 6.5 mmol kg^{-1} in the three permeates. The evolution of total and soluble lactate ions during concentration were added to the graphs (Fig. 5) because lactate ions, by association with calcium, could form calcium lactate salt. The latter has a solubility limit of 4.08 g of anhydrous calcium lactate per 100 g of water at $25 \text{ }^\circ\text{C}$ and 17.94 g at $60 \text{ }^\circ\text{C}$ (Kubantseva & Hartel, 2002).

For P-AL1, the experimental results evidenced a predominant precipitation of calcium phosphate salt in the concentrates from the start of concentration. Citrate ions remained mostly soluble throughout the concentration process, except at a high dry matter content (over $350\text{--}400 \text{ g kg}^{-1}$ DM). Lastly, lactate ions remained completely soluble in the concentrates within the range of the CF values studied. According to the MilkSalt GLM software and at pH 6.3, calcium ions existed mainly as a complex of CaCit^- and as free Ca^{2+} ions in the initial permeate. Only a very small part was associated with phosphate, chloride or lactate, the latter being mostly free ions. The determination of salt equilibria using the MilkSalt GLM software indicated that calcium phosphate was at the edge of precipitation. Then, as soon as P-AL1 was concentrated, calcium phosphate precipitated because the amount of phosphate ion in the form of HPO_4^{2-} predominated over Cit^{3-} . The reduction in pH during concentration tended to protonate HPO_4^{2-} into H_2PO_4^- and favoured the slow co-precipitation of calcium citrate (Ca_3Cit_2), thus explaining the presence of citrate in the precipitate of P-AL1 at the

higher CF. At CF 10.8, the experimental results and the theoretical values provided by the software were quite similar. From the experiments, 95 mM of calcium and 52 mM of phosphate were precipitated, close to the theoretical values of 93 and 51 mM, respectively. Moreover, the software calculated a high saturation index for calcium citrate salt, which confirmed that some calcium citrate could be precipitated.

As for P-AL1, calcium phosphate precipitation occurred in the P-AL-2 concentrates but to a lesser extent and from a higher DM content (about 300 g kg⁻¹). In experimental set #1, the evolution of the citrate ion content during concentration evidenced precipitation (i) from the same DM content as for calcium and phosphate ions, (ii) at a total citrate content close to 40 mmol kg⁻¹, the threshold previously evidenced during P-ACit and P-ACI concentrations and (iii) in large quantities as the proportion of insoluble citrate reached 54.9% in the concentrate at 452.4 g kg⁻¹ DM. Surprisingly, the results for experimental set #2 showed a linear evolution of the soluble citrate ion content as a function of the DM content of concentrates. A supplementary analysis of a P-AL2 sample concentrated at 407.8 g kg⁻¹ DM confirmed the findings regarding experimental set #2; the soluble citrate ion content of 51.6 mmol kg⁻¹ reached a calculated total content of 57.4 mmol kg⁻¹. This discrepancy between experimental sets could be explained by the long induction period required for calcium citrate precipitation and/or the formation of lactose crystals during P-AL permeate concentration (see above); the latter constituted "impurities" that initiated the random crystallisation of calcium citrate salt in some samples.

Based on MilkSalt GLM software, the predicted calcium speciation in initial P-AL2 at pH 5.25 indicated that calcium was mainly present as free ions (50%), and the other fraction was under soluble complexes, mainly CaCit⁻, CaLact⁻ (16% and 18%, respectively) and to a lesser extent associated with inorganic phosphate (H₂PO₄⁻: 5.6%; HPO₄²⁻: 2%), chloride (5%) and HClit²⁻ (2.4%). Calcium phosphate was below its solubility limit which explains why its precipitation was shifted to the higher CF in comparison with P-AL1. For the higher concentrated product at FC 12.7, the software indicated 119 mM calcium and 65 mM inorganic phosphate were precipitated, whereas the experimental results evidenced 116 mM and 84 mM, respectively. Further, the calculated saturation ratio for calcium citrate salt was evaluated at 54, which would indicate the likelihood of calcium citrate precipitation. Interestingly, the software also indicated that around 22% of total calcium was associated with lactate ions, which reduced the ionic calcium available and the likelihood of the precipitation of calcium citrate and calcium phosphate.

The experimental results showed that few calcium precipitates were formed throughout P-AL3 concentration and they only appeared at higher CF values. Based on the MilkSalt GLM software, the predicted calcium speciation in initial P-AL3 at pH 4.63 indicated that calcium existed mainly as free ions (50%), and as CaLact⁻ (23%) and CaCit⁻ (9.4%) soluble complexes. It was also associated to a lesser extent with H₂PO₄⁻ (5.9%), HClit²⁻ (5.8%) and chloride (4.7%). Several parameters contributed to the small quantity of calcium salts formed during P-AL3 concentration: (i) formation of the CaLact⁻ complex that reduced the amount of ionic calcium available for potential associations with citrate and phosphate, (ii) the higher solubility of calcium lactate salt compared with calcium phosphate solubility, (iii) the high lactate content, (iv) the low citrate content compared with lactate and phosphate contents, and (v) the ionic form of phosphate within the range 4.63 to 4.23 (H₂PO₄⁻) that has a low affinity for calcium (12 M⁻¹ (Holt, Dalgleish, & Jenness, 1981)). The presence of lactate ions displaced the equilibrium in the calcium-phosphate-citrate system towards the

formation of calcium lactate, thus inhibiting the precipitation of calcium citrate and calcium phosphate.

For a comparison, Tanguy et al. (2019) performed the vacuum concentration of an industrial lactic acid whey using a pilot-scale falling-film evaporator and studied the evolution of total and soluble ion contents during concentration. The lactic acid whey was a by-product of industrial fresh cheese production, which was characterised by a large quantity of lactate ions (109.8 mmol kg⁻¹) and an absence of citrate ions, which were consumed by lactic bacteria during cheese processing. The authors evidenced an absence of precipitation in the lactic acid whey concentrates and explained this result by the presence of lactate. Similarly, and in the context of producing lactic acid whey powders, Mimouni (2007) showed that the addition of sodium citrate to industrial lactic acid whey concentrates was a means to reduce the formation of calcium lactate crystals, which are responsible for a thickening of concentrates during lactose crystallisation.

4. Conclusion

This work investigated the influence of mineral composition and pH on the nature and amount of minerals that precipitate in concentrates during whey concentration. Dairy ultrafiltration permeates with variable mineral compositions and pH values were prepared by the ultrafiltration of non-acidified and acidified milk using different acids. Depending on the permeates considered and the CF, the results evidenced either some precipitation of calcium salts (calcium phosphate, calcium citrate) in the concentrates, or no precipitation. Calcium phosphate was the dominant mineral species in the precipitate of concentrates in which the main ionic form of inorganic phosphate was HPO₄²⁻. This was the case of concentrates obtained by the concentration of PUF at pH 6.7 and P-AL1 at pH 6.3. At a pH of around 5.0, the high affinity between calcium ions and Cit³⁻, and the reduced affinity of phosphate for calcium, favoured the precipitation of calcium citrate. However, the degree of precipitation could be limited because insufficient Cit³⁻ was present to exceed the solubility limit of calcium citrate.

Calcium citrate precipitation occurred extensively in concentrates resulting from the concentration of P-ACit at pH 5.6 due to the large quantity of citrate ions (both initial and added). It also took place in P-ACI concentrates, but at a higher CF because of the smaller quantities of citrate ions. Lastly, the large quantities of lactate ions in the P-AL2 and P-AL3 concentrates modified the ion equilibrium and particularly the calcium-citrate-phosphate system. It reduced the quantity of ionic calcium available for further association with citrate and phosphate ions, inhibiting the precipitation of calcium citrate and calcium phosphate. However, lactate ions promoted lactose crystallisation in the concentrates.

During permeate concentration, the affinity between calcium and the main anions (phosphate, citrate and lactate) and the amounts of each species determine the likelihood of the precipitation of salts. The behaviour of these ions during concentration can be assessed in light of: (i) the nature and quantities of ions available in the concentrates, (ii) the anionic forms present at the pH of the concentrates and their association constants with calcium, and (iii) the solubility limit of calcium salts. The next stage in this work will be to study the influence of the whey proteins present in industrial whey on calcium salt precipitation.

Funding

This research did not receive any specific grant from funding agencies in the public, commercial, or not-for-profit sectors.

Declaration of competing interest

None.

References

- Daufin, G., & Labbé, J.-P. (1998). Equipment fouling in the dairy application : Problem and pretreatment. In Z. Amjad (Ed.), *Calcium phosphates in biological and industrial systems* (pp. 437–463). New York, NY, USA: Springer.
- De Wit, J. N. (2001). *Lecturer's handbook on whey and whey products* (1st ed.). Brussels, Belgium: European Whey Products Association.
- de Jong, P. (1997). Impact and control of fouling in milk processing. *Trends in Food Science & Technology*, 8, 401–405.
- Ganju, S., & Gogate, P. R. (2017). A review on approaches for efficient recovery of whey proteins from dairy industry effluents. *Journal of Food Engineering*, 215(Supplement C), 84–96.
- Gao, R., van Halsema, F. E. D., Temminghoff, E. J. M., van Leeuwen, H. P., van Valenberg, H. J. F., Eisner, M. D., et al. (2010). Modelling ion composition in simulated milk ultrafiltrate (SMUF). I : Influence of calcium phosphate precipitation. *Food Chemistry*, 122, 700–709.
- García, A. C., Vavrusova, M., & Skibsted, L. H. (2018). Supersaturation of calcium citrate as a mechanism behind enhanced availability of calcium phosphates by presence of citrate. *Food Research International*, 107, 195–205.
- Gaucheron, F. (2005). The minerals of milk. *Reproduction Nutrition Development*, 45, 473–483.
- Gaucheron, F., Le Graët, Y., Piot, M., & Boyaval, E. (1996). Determination of anions of milk by ion chromatography. *Le Lait*, 76, 433–443.
- Gernigon, G., Baillon, F., Espitalier, F., Le Floch-Fouere, C., Schuck, P., & Jeantet, R. (2013). Effects of the addition of various minerals, proteins and salts of organic acids on the principal steps of alpha-lactose monohydrate crystallisation. *International Dairy Journal*, 30, 88–95.
- Holt, C., Dalgleish, D. G., & Jenness, R. (1981). Calculation of the ion equilibria in milk diffusate and comparison with experiment. *Analytical Biochemistry*, 113, 154–163.
- ISO-IDF. (1964). *International Standard 27—determination of the ash content of processed cheese product*. Brussels, Belgium: International Dairy Federation.
- ISO-IDF. (1987). *International Standard 21B - milk, cream and evaporated milk : Determination of total solids content*. Brussels, Belgium: International Dairy Federation.
- ISO-IDF. (1993). *International standard 20B - milk : Determination of nitrogen content*. Brussels, Belgium: International Dairy Federation.
- Jeurnink, T. J. M., & Brinkman, D. W. (1994). The cleaning of heat exchangers and evaporators after processing milk or whey. *International Dairy Journal*, 4, 347–368.
- Kessler, H. G. (1986). Multistage evaporation and water vapour recompression with special emphasis on high dry matter content, product losses, cleaning and energy savings. *Milk – the Vital Force, proceedings of the 22nd international dairy congress*, 545–558.
- Kubantseva, N., & Hartel, R. W. (2002). Solubility of calcium lactate in aqueous solution. *Food Reviews International*, 18, 135–149.
- Le Graët, Y., & Brule, G. (1993). Effects of pH and ionic-strength on distribution of mineral salts in milk. *Le Lait*, 73, 51–60.
- Liu, X.-C., Kirkensgaard, J. J. K., & Skibsted, L. H. (2021). Hydrates of calcium citrate and their interconversion in relation to calcium bioaccessibility. *Food Research International*, 140, Article 109867.
- Mekmene, O., Le Graët, Y., & Gaucheron, F. (2009). A model for predicting salt equilibria in milk and mineral-enriched milks. *Food Chemistry*, 116, 233–239.
- Mekmene, O., Le Graët, Y., & Gaucheron, F. (2010). Theoretical model for calculating ionic equilibria in milk as a function of pH : Comparison to experiment. *Journal of Agricultural and Food Chemistry*, 58, 4440–4447.
- Mekmene, O., Leconte, N., Rouillon, T., Quillard, S., Bouler, J. M., & Gaucheron, F. (2012). Physicochemical characterisation of calcium phosphates prepared from milk ultrafiltrates : Effect of the mineral composition. *International Journal of Dairy Technology*, 65, 334–341.
- Mimouni, A. (2007). *Cristallisation du lactose et épaississement dans les lactosérums concentrés*. Rennes, France: Ecole Nationale Supérieure d'Agronomie de Rennes (PhD thesis).
- Morison, K. R. (2015). Reduction of fouling in falling-film evaporators by design. *Food and Bioprocess Technology*, 93, 211–216.
- Pearce, R. J. (1992). Whey processing. In J. G. Zadow (Ed.), *Whey and lactose processing* (pp. 73–99). Dordrecht, Netherlands: Springer.
- Resmini, P., Pellegrino, L., Andreini, R., & Prati, F. (1989). Determinazione delle sieroproteine solubili del latte per HPLC (cromatografia liquida ad alta prestazione) in fase inversa. *Scienza e Technica Lattario-casearia*, 40, 7–23.
- Rice, G., Barber, A., O'Connor, A., Stevens, G., & Kentish, S. (2010). A theoretical and experimental analysis of calcium speciation and precipitation in dairy ultrafiltration permeate. *International Dairy Journal*, 20, 694–706.
- Saulnier, F., Calco, M., Humbert, G., & Linden, G. (1996). Organic and mineral composition from industrial acid wheys analysed by capillary electrophoresis. *Le Lait*, 76, 423–432.
- Schmidt, R., Packard, V., & Morris, H. (1984). Effect of processing on whey-protein functionality. *Journal of Dairy Science*, 67, 2723–2733.
- Schuck, P., Bouhallab, S., Durupt, D., Vareille, P., Humbert, J.-P., & Marin, M. (2004). Séchage des lactosérums et dérivés : Rôle du lactose et de la dynamique de l'eau. *Le Lait*, 84, 243–268.
- Singh, H., & Newstead, D. F. (1992). Aspects of protein in milk powder manufacture. In P. F. Fox (Ed.), *Advanced dairy chemistry* (Vol. 1, pp. 621–656). London, UK: Elsevier Science Publishers. Proteins.
- Smart, J. B., & Smith, J. M. (1992). Effect of selected compounds on the rate of α -lactose monohydrate crystallization, crystal yield and quality. *International Dairy Journal*, 2, 41–53.
- Smithers, G. W. (2008). Whey and whey proteins—from 'gutter-to-gold'. *International Dairy Journal*, 18, 695–704.
- Tanguy, G., Siddique, F., Beaucher, E., Santellani, A.-C., Schuck, P., & Gaucheron, F. (2016). Calcium phosphate precipitation during concentration by vacuum evaporation of milk ultrafiltrate and microfiltrate. *Lebensmittel-Wissenschaft und -Technologie- Food Science and Technology*, 69, 554–562.
- Tanguy, G., Tuler-Perrone, I., Dolivet, A., Santellani, A. C., Leduc, A., Jeantet, R., et al. (2019). Calcium citrate insolubilization drives the fouling of falling film evaporators during the concentration of hydrochloric acid whey. *Food Research International*, 116, 175–183.
- Vavrusova, M., Garcia, A., P. Danielsen, B., & H. Skibsted, L. (2017b). Spontaneous supersaturation of calcium citrate from simultaneous isothermal dissolution of sodium citrate and sparingly soluble calcium hydroxycarboxylates in water. *RSC Advances*, 7, 3078–3088.
- Vavrusova, M., Johansen, N. P., Garcia, A. C., & Skibsted, L. H. (2017a). Aqueous citric acid as a promising cleaning agent of whey evaporators. *International Dairy Journal*, 69, 45–50.
- Walstra, P., Wouters, J. T. M., & Guerts, T. J. (2006). *Dairy science and technology* (2nd ed.). Boca Raton, FL, USA: CRC Press.
- Wijayasinghe, R., Vasiljevic, T., & Chandrapala, J. (2016). Lactose behaviour in the presence of lactic acid and calcium. *Journal of Dairy Research*, 83, 395–401.
- Zall, R. R. (1992). Sources and composition of whey and permeate. In J. G. Zadow (Ed.), *Whey and lactose processing* (pp. 1–72). Dordrecht, Netherlands: Springer.